FULL PAPER

Dalton
www.rsc.org/dalton

The nature of aryloxide and arylsulfide ligand bonding in dimethyltitanium complexes containing cyclopentadienyl ligation†

Thomas A. Manz,[a] Andrew E. Fenwick,[b] Khamphee Phomphrai,[b] Ian P. Rothwell‡[b] and Kendall T. Thomson*[a]

[a] *School of Chemical Engineering, Purdue University, West Lafayette, IN 47907, USA. E-mail: thomsonk@purdue.edu*

[b] *Department of Chemistry, Purdue University, West Lafayette, IN 47907, USA*

Received 12th August 2004, Accepted 17th December 2004
First published as an Advance Article on the web 21st January 2005

A series of dimethyltitanium compounds [CpTi(EAr)Me_2] (E = O, S) ligated by one cyclopentadienyl (Cp) and one aryloxide (OAr) or arylsulfide (SAr) have been structurally characterized in order to gain a better understanding of aryloxide and arylsulfide bonding in these systems. Experimental structures were compared to those predicted by density functional theory (DFT). Bonding in the arylsulfide systems was found to be significantly different from bonding in the aryloxide systems. The aryloxide ligands exhibited wide Ti–O–Ar angles (≥150°) with the Ar group oriented proximal to the Cp group. DFT computations revealed two conformers for the arylsulfide systems. Arylsulfides with the Ar group proximal to the Cp group had a predicted Ti–S–Ar angle of ~120° while those with the Ar group distal to the Cp group had a measured and predicted Ti–S–Ar angle of ~100°. Molecular and natural bond orbital (NBO) analyses were employed to explain the nature of ligand bonding in these systems.

Introduction

Cyclopentadienyl (Cp) ligation is ubiquitous in group 4 organometallic chemistry. Since the introduction of Cp_2TiCl_2 in 1953,[1,2] the broad applicability of titanocenes has been studied for derivatives containing a range of alkyl, aryl, and heteroatom-substituted Cp rings, as well as *ansa*-titanocenes that have the two Cp rings linked by a bridging group.[3] The innovation of modified titanocenes has motivated research into the development of mono-Cp derivatives that contain a different anionic ligand. Non-bridged half-metallocene group 4 transition metal complexes of the type, Cp′M(L)X_2 (Cp′ = cyclopentadienyl group; M = Ti, Zr, Hf; L = anionic ligand such as OAr, NR_2, NPR_3, *etc.*; X = halogen, alkyl) have been studied, and many complement metallocene-type and "constrained geometry" systems.[3] In addition, subtle changes within specific ligand types have been demonstrated to effect a significant change in the environment around the metal center, as observed in the reactivity.[4]

Bis(aryloxide) titanium and zirconium compounds of the type [$(ArO)_2MR_2$] (R = Me, CH_2Ph) have been thoroughly studied.[5,6] The aryloxide ligand can adopt a bonding motif isolobal with that of cyclopentadienyl, potentially bonding in a $\sigma^2\pi^4$ fashion. A key property of these ligands is their tunability, as a wide collection of phenols offering a unique and diverse set of steric and electronic alternatives are commercially available or can be readily synthesized. This has provided both novel and complementary chemistry to the well-studied metallocenes.

The introduction of these compounds has been followed by the development of mixed-cyclopentadienyl/aryloxide [CpTi(OAr)Cl_2] systems, which have been structurally compared to the related metallocene [Cp_2TiCl_2] and bis(aryloxide) [$(ArO)_2TiCl_2$] systems.[7,8] In addition, dialkyl derivatives of the type [CpTi(OAr)R_2] (R = Me, CH_2Ph) have recently been reported.[5,9] A detailed study of the formation and decomposition of monomethyl cationic derivatives formed when the dimethyl compounds were activated by a Lewis acidic borane was included in the study. These cationic derivatives have been demonstrated to function as single-site catalysts for the polymerization of olefins such as 1-hexene and styrene.[10]

To extend our study of the effects of aryloxide on structure and reactivity, we began investigating the related arylsulfide chemistry.[11] Many substituted arylthiols are known and can function as ligands that meet a variety of steric and electronic requirements.[12–17] There are several prior studies involving titanium compounds that contain arylsulfide ligands, and several crystal structures have been reported. Given the abundance of CpTi(OAr)R_2 complexes, we are not aware of any examples of CpTi(SAr)R_2 analogues being synthesized or characterized. Herein, some CpTi(SAr)Me_2 complexes have been synthesized and X-ray crystal structures have been reported. DFT calculations have been performed and Ti–S bonding is compared with CpTi(OAr)Me_2 complexes.

Experimental

General details

All operations were carried out under a dry nitrogen atmosphere using standard Schlenk techniques. The hydrocarbon solvents were purified employing Grubbs-type column systems manufactured by Innovative Technologies, and were stored over sodium ribbons under nitrogen until use. The synthesis and X-ray structure of [CpTi($OC_6H_2Me_2$-2,6-Br-4)Me_2] has been previously reported,[9] and a similar procedure was followed for the preparation of the arylsulfide analogues. The syntheses of [$CpTiCl_3$][18] and 2,4,6-trialkylbenzenethiols[13] were performed according to literature procedures or slight variations thereof. All other reagents were purchased from Aldrich and used without further purification. The ^1H and ^{13}C NMR spectra were obtained on a Varian Associates Inova-300 spectrometer and referenced to the protio impurity of commercial benzene-d_6 (C_6D_6) as an internal standard. Elemental analyses and X-ray diffraction studies were performed in-house at Purdue University.

† Electronic supplementary information (ESI) available: (1) DFT optimized geometries. (2) Synthesis procedure and ORTEP drawing for compound **2**. (3) Comparison of structural parameters computed from different basis sets (6-311+G and 6-311++G**) and exchange–correlation functionals (OLYP and B3LYP). See http://www.rsc.org/suppdata/dt/b4/b412455c/

‡ This paper is dedicated to the memory of Ian P. Rothwell, Richard B. Moore Distinguished Professor of Chemistry.

DOI: 10.1039/b412455c

Table 1 Crystal data and data collection parameters

Compound	[CpTi($SC_6H_2Me_3$-2,4,6)Me_2]	[CpTi($SC_6H_2Pr^i_3$-2,4,6)Me_2]
Formula	$C_{16}H_{22}STi$	$C_{22}H_{34}STi$
M_r	294.32	378.48
Space group	$P\bar{1}$ (no. 2)	$C2$ (no. 5)
a/Å	6.947(1)	32.440(3)
b/Å	7.887(1)	8.3708(3)
c/Å	15.038(2)	15.978(1)
α/°	75.487(8)	90
β/°	80.377(7)	102.68(3)
γ/°	80.912(9)	90
V/Å^3	780.6(2)	4232.9(5)
Z	2	8
D_c/g cm^{-3}	1.252	1.188
T/K	150.	150.
Radiation (λ/Å)	Mo-Kα (0.71073)	Mo-Kα (0.71073)
R	0.045	0.077
R_w	0.123	0.187

[CpTi($SC_6H_2Me_3$-2,4,6)Me_2] (1)

A suspension of [$CpTiCl_3$] (2.00 g, 9.12 mmol in 50 mL Et_2O) was cooled to −78 °C in a dry ice/acetone bath. To this suspension was added [LiMe] (17.1 mL, 1.6 M in diethyl ether, 27.4 mmol) *via* syringe under a flush of nitrogen. After stirring for approximately 4 h, a solution of 2,4,6-trimethylbenzenethiol (1.39 g, 9.12 mmol in 20 mL Et_2O) was added dropwise at −78 °C. The mixture was allowed to slowly warm to room temperature and was stirred overnight. The solvent was removed under vacuum, and benzene was added to the residue. The suspension was filtered through a plug of Celite over fritted glass to remove the lithium salts. The filtrate was then evacuated to dryness yielding a dark yellow oil. The oil was dissolved in 5 mL hexane and cooled to −20 °C, yielding X-ray quality crystals (1.89 g, 71%). Anal. Calc. for $C_{16}H_{22}STi$: C, 65.30; H, 7.54; S, 10.90. Found: C, 65.06; H, 7.40; S, 10.62%. ^{1}H NMR (C_6D_6, 25 °C): δ 7.01 (s, *m*-H); 5.96 (s, Cp); 2.48 (s, *o*-Me); 2.20 (s, *p*-Me); 0.97 (s, Ti-Me). ^{13}C NMR (C_6D_6, 25 °C): δ 140.7, 137.0, 136.2, 129.7 (aromatics); 114.4 (Cp); 66.8 (Ti-Me); 23.5 (*o*-Me); 21.1 (*p*-Me).

A similar procedure was used to synthesize [CpTi($SC_6H_2Pr^i_3$-2,4,6)Me_2] (**2**). Full details are found in the ESI.†

Density functional theory calculations

DFT calculations were performed in Gaussian 03[19] using the B3LYP exchange–correlation functional, the 6-311++G** basis set, auto density fitting, the gdiis geometry optimization algorithm, and default convergence criteria.[20] Dependence of the calculated energies and geometries on the basis set size and exchange–correlation functional were also investigated. Energies and geometries using the OLYP[21–23] exchange–correlation functional and 6-311+G basis set are reported in the ESI† for comparison purposes. Use of the OLYP exchange–correlation functional was found to provide significant speed-up compared to the B3LYP functional while still providing good accuracy. For the energy minimum and transition state structures, forces were converged to better than 0.00045 a.u. and atom displacements were converged to better than 0.0018 a.u. For the constrained Ti–E–Ar angle calculations, forces were converged to better than 0.0017 a.u. and atom displacements were converged to better than 0.01 a.u. The QST3 method was utilized to find the transition state for interconversion between proximal and distal conformations of [CpTi($SC_6H_2Me_3$-2,4,6)Me_2].

X-Ray data collection and reduction

Crystal data and data collection parameters are contained in Table 1. A suitable crystal was mounted on a glass fiber in a random orientation under a cold stream of dry nitrogen. Preliminary examination and final data collection were performed with Mo-Kα radiation (λ = 0.71073 Å) on a Nonius Kappa CCD. Lorentz and polarization corrections were applied to the data.[24] An empirical absorption correction using SCALEPACK was applied.[25] Intensities of equivalent reflections were averaged. The structure was solved using the structure solution program PATTY in DIRDIF92.[26] The remaining atoms were located in succeeding difference Fourier syntheses. Hydrogen atoms were included in the refinement but restrained to ride on the atom to which they are bonded. The structure was refined in full-matrix least-squares where the function minimized was $\Sigma w(|F_o|^2 - |F_c|^2)^2$ and the weight w is defined as $w = 1/[\sigma^2(F_o^2) + (0.0585P)^2 + 1.4064P]$ where $P = (F_o^2 + 2F_c^2)/3$. Scattering factors were taken from the *International Tables for Crystallography*.[27] Refinement was performed on an AlphaServer 2100 using SHELX-97.[28] Crystallographic drawings were created using ORTEP-3 for Windows version 1.076.[29] The crystal structure of compound **2** is disordered at the *para*-isopropyl group. Default SHELX restraints were used in the refinement. The largest residual electron density peak is located 1.48 Å from C(112).

CCDC reference numbers 247467 and 247468.

See http://www.rsc.org/suppdata/dt/b4/b412455c/ for crystallographic data in CIF or other electronic format.

Results and discussion

Synthesis and characterization

Synthesis of the mixed-cyclopentadienyl/arylsulfide compounds was attempted using two methods employed successfully for the aryloxide analogues. In the first method, LiSAr was added to a solution of $CpTiCl_3$ in benzene giving $CpTi(SAr)Cl_2$. A subsequent methylation of the corresponding dichloride $CpTi(SAr)Cl_2$ with two equivalents of methyllithium or MeMgCl gave $CpTi(SAr)Me_2$ (Scheme 1(a)). Although the products typically could be observed in the reaction mixture *vide infra*, attempts to isolate pure products from the reaction mixture were unsuccessful, yielding dark brown, viscous residues regardless of reaction solvent and temperature. In the second and preferred method, the dimethyl complexes $CpTi(SAr)Me_2$ were synthesized directly from $CpTiCl_3$ using a one-pot procedure

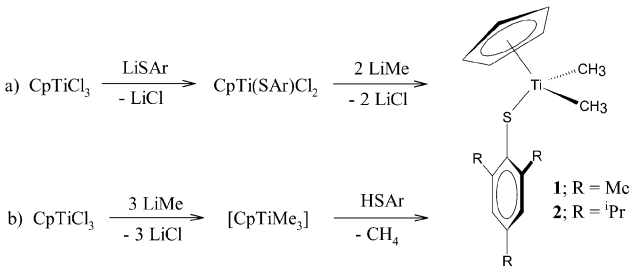

Scheme 1

Table 2 Structural parameters for [CpTi(EAr)X_2]; EAr = OAr, SAr; X = Cl, Me

Compound	Ti–X/Å	Ti–Cp/Å	Ti–E/Å	E–Ti–X/°	X–Ti–X/°	Cp–Ti–X/°	Ti–E–C/°
[CpTi($OC_6H_2Me_2$-2,6-Br-4)Me_2][a]	2.088(2), 2.101(2)	2.046(2)	1.812(1)	103.64(8), 103.72(7)	100.80(9)	112.91(9), 113.21(9)	150.0(1)
[CpTi($OC_6H_3Pr^i_2$-2,6)Me_2][a]	2.103(3), 2.105(3)	2.045(3)	1.803(2)	104.0(1), 103.2(1)	101.8(1)	112.4(1), 112.6(1)	157.5(1)
[CpTi($SC_6H_2Me_3$-2,4,6)Cl_2][b]	2.2522(8), 2.2557(7)	2.017(2)	2.2912(7)	106.71(3), 107.60(3)	101.59(3)	118.48(8), 117.09(7)	106.55(7)
[CpTi($SC_6H_2Pr^i_3$-2,4,6)Cl_2][b]	2.251(1), 2.240(1)	2.026(5)	2.287(1)	106.98(5), 106.01(5)	102.92(5)	117.2(2), 115.9(2)	96.9(2)
[CpTi($SC_6H_2Me_3$-2,4,6)Me_2] (**1**)	2.105(2), 2.142(2)	2.040(3)	2.3242(8)	109.74(7), 107.62(6)	100.2(1)	113.2(1), 114.3(1)	99.78(7)
[CpTi($SC_6H_2Pr^i_3$-2,4,6)Me_2] (**2**)	2.072(9), 2.061(8)	2.032(8)	2.325(2)	109.3(3), 108.5(3)	97.3(4)	114.9(3), 115.3(3)	102.5(2)

[a] Data taken from ref. 9. [b] Data taken from ref. 11.

in which [$CpTiMe_3$] was generated *in situ* at −78 °C, followed by the addition of HSAr at −78 °C to form CpTi(SAr)Me_2 (Scheme 1(b)). This method allowed for the isolation of pure crystalline product in high yield. However, slow decomposition of the isolated solid was observed over days at room temperature.

The ^{1}H and ^{13}C NMR spectra of **1** and **2** were uncomplicated, with one Cp, one methyl, and a single set of arylsulfide resonances in each case. The Cp protons were observed approximately 0.2 ppm upfield relative to their dichloro analogues, reflecting the decrease in electrophilicity of the metal center as chloride atoms are replaced by methyl groups.

Compounds **1** and **2** have been analyzed by X-ray crystallography (Table 1) and the ORTEP drawing of compound **1** is represented in Fig. 1. The dimethyl compounds exhibit a pseudo-tetrahedral geometry about the metal center. The Ti–S–Ar bond angle in **2** is bigger than in **1** likely due to the steric hindrance of ^{i}Pr groups. Selected structural parameters, along with those for closely related [CpTi(EAr)X_2] derivatives (EAr = OAr, SAr; X = Cl, Me) are collected in Table 2. Very little difference is observed in the structural parameters of these somewhat distinct systems. Noteworthy is the shorter Ti–Cp distance in the dichlorides relative to the aryloxo and arylsulfide dimethyl compounds. In addition, the Ti–S–C bond angles are significantly smaller than the Ti–O–C bond angles in the analogous systems. The larger Ti–S–C bond angle observed in these systems is under 107°, while the smaller Ti–O–C angle is 150°.

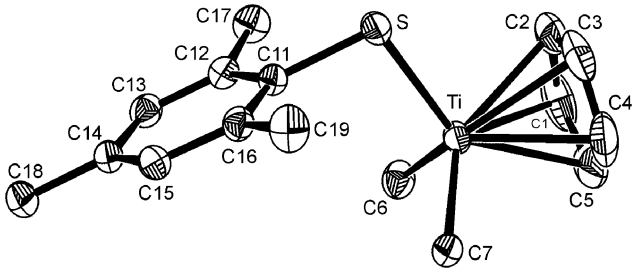

Fig. 1 ORTEP drawing (50% thermal ellipsoids) of CpTi($SC_6H_2Me_3$-2,4,6)Me_2, **1**.

DFT Calculation

Table 3 compares bond lengths and angles in the crystalline state obtained by X-ray diffraction to those predicted theoretically

Table 3 Selected bond distances (Å) and angles (°)

			[CpTi($SC_6H_2Me_3$-2,4,6)Me_2][b]	
	[CpTi($OC_6H_2Me_2$-2,6-Br-4)Me_2][a]	[CpTi($OC_6H_3Me_2$-2,6)Me_2]	Distal	proximal
Ti–E[c]	1.812(1)[d]		2.3242(8)	
	[1.8153][e]	[1.8110]	[2.3506]	[2.3431]
Ti–C(6)	2.088(2)		2.105(2)	
	[2.1111]	[2.1121]	[2.1003]	[2.1000]
Ti–C(7)	2.101(2)		2.142(2)	
	[2.1111]	[2.1121]	[2.1003]	[2.1012]
Ti–Cp	2.046(2)		2.040(3)	
	[2.09]	[2.10]	[2.08]	[2.06]
E–Ti–Cp	120.29(9)		111.1(1)	
	[123.7]	[123.4]	[111.5]	[120.8]
E–Ti–C(6)	103.64(8)		107.62(6)	
	[103.3]	[103.5]	[109.0]	[103.1]
E–Ti–C(7)	103.72(7)		109.74(7)	
	[103.3]	[103.5]	[109.0]	[103.2]
Ti–E–C(11)	150.0(1)		99.78(7)	
	[167.0]	[165.7]	[103.4]	[117.1]
C(6)-Ti–C(7)	100.80(9)		100.2(1)	
	[99.9]	[99.9]	[99.5]	[100.3]
C(6)-Ti–Cp	112.91(9)		113.2(1)	
	[111.8]	[111.8]	[113.6]	[113.4]
C(7)-Ti–Cp	113.21(9)		114.3(1)	
	[111.9]	[111.9]	[113.6]	[113.4]

[a] Data taken from ref. 9. [b] Conformer with ArS distal or proximal to Cp ring. [c] E = O or S. [d] Experimental values (X-ray crystallography). [e] DFT calculation (B3LYP/6-311++G**).

from density functional theory (DFT) using the B3LYP functional and 6-311++G** basis set. From the calculations, a single configuration was observed for the aryloxide compounds, whereas two configurations were observed for each of the arylsulfide compounds (Scheme 2). In the proximal configuration, the arylsulfide group bends toward the Cp group. In the distal configuration the arylsulfide group bends away from the Cp group. According to the DFT calculations, the distal conformation of compound **1** is lower in energy than the proximal conformation by 5.25 kJ mol^{-1}. The calculated structural parameters for the distal conformation are in good agreement with those found in the solid state.

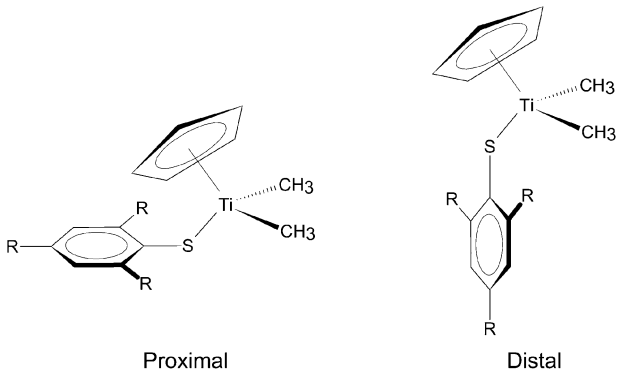

Scheme 2

The Ti–O–Ar bond angles were found to be very wide (≥150°) whereas the Ti–S–Ar bond angles were found to be slightly less than tetrahedral (~100°) in the distal conformation and greater than tetrahedral (~120°) in the proximal conformation. The large difference between Ti–O–Ar and Ti–S–Ar bond angle suggests a significant change in underlying bonding between aryloxide and arylsulfide ligands in these systems.

Additionally, the Ti–O distance (~1.81 Å) is much shorter than the Ti–S distance (~2.33 Å). This is primarily due to the larger radius of the S atom compared to the O atom. The atomic radii of Ti, S, and O are approximately 1.40, 1.00, and 0.60 Å, respectively.[30] The sum of the atomic radii of Ti and S gives 2.40, while that of Ti and O gives 2.00 Å. The Ti–O and Ti–S bond lengths were found to be shorter than would be predicted by the sum of atomic radii. This effect is more pronounced in the aryloxide compounds,[31,32] and is believed to indicate the extent of π-bonding to the metal center.[32]

A few computations were done to investigate the choice of basis set and exchange–correlation functional on the accuracy of the computed structural parameters. The OLYP and B3LYP functionals and the 6-311+G and 6-311++G** basis sets were used to compute the structural parameters of distal [CpTi($SC_6H_2Me_3$-2,4,6)Me_2] which were compared to the experimental values. Use of the OLYP functional was found to give significant speed-up compared to B3LYP with a slight loss in accuracy. The largest change was for the Ti–S bond distance which had values of 2.3966 (OLYP/6-311 + G), 2.3716 (OLYP/6-311++G**), 2.3717 (B3LYP/6-311+G), and 2.35058 (B3LYP/6-311++G**) compared to the experimental bond distance of 2.3242 Å. The Ti–S–C bond angle followed a similar trend, having values of 107.4 (OLYP/6-311+G), 106.5 (OLYP/6-311++G**), 103.8 (B3LYP/6-311+G), and 103.4 (B3LYP/6-311++G**) compared to the experimental bond angle of 99.8°. All of the other bond distances and angles changed by amounts smaller than these. The B3LYP functional with 6-311++G** basis set was used for the molecular orbital and bonding analysis presented below.

Frontier molecular orbitals

Figs. 2–4 show the HOMO of arylsulfides, distal [CpTi($SC_6H_2Me_3$-2,4,6)Me_2] and proximal [CpTi($SC_6H_2Me_3$-2,4,6)Me_2], and the aryloxide [CpTi($OC_6H_3Me_2$-2,6)Me_2], respectively. Positive values of the molecular orbital are illustrated in red while negative values are illustrated in green (the plots are 0.02 isosurfaces). In each of the compounds, the *z*-axis is along the Ti–O or Ti–S bond, the *x*-axis is perpendicular to the *z*-axis and lies in the plane of the phenyl ring, and the *y*-axis is perpendicular to the *xz*-plane.

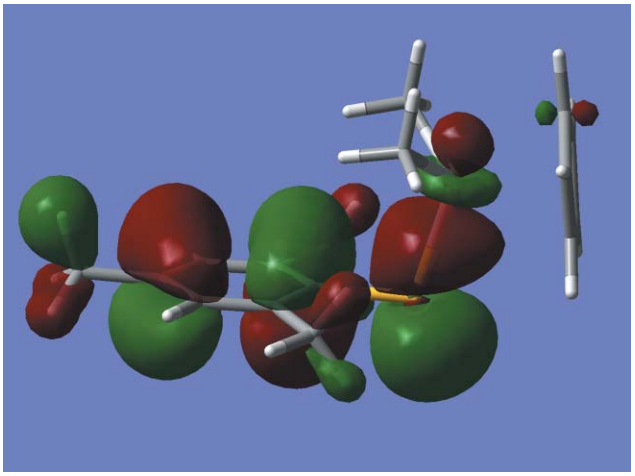

Fig. 2 HOMO of distal [CpTi($SC_6H_2Me_3$-2,4,6)Me_2] showing overlap of the sulfur p_z orbital with the titanium d_{z^2} orbital.

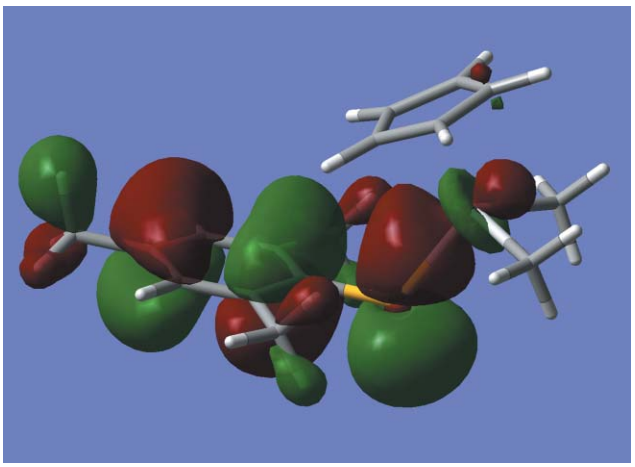

Fig. 3 HOMO of proximal [CpTi($SC_6H_2Me_3$-2,4,6)Me_2].

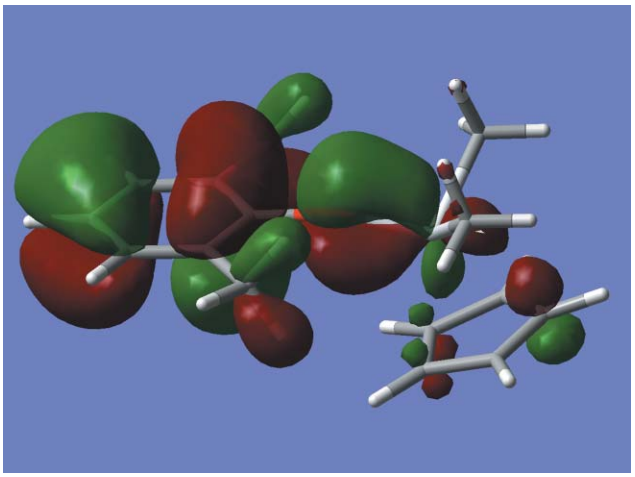

Fig. 4 HOMO of [CpTi($OC_6H_3Me_2$-2,6)Me_2] showing overlap of the oxygen p_y orbital with the titanium d_{yz} orbital.

In the distal arylsulfide HOMO (molecular orbital # 78) shown in Fig. 2, the σ-bonding between the sulfur p_z orbital and the coaxial d_{z^2} orbital on titanium is evident. The HOMO also includes anti-bonding interaction of the phenyl ring π_2 (e_{1g}) orbital with s-orbitals of periphery methyl hydrogens bound to the phenyl ring. The methyl groups bound to the titanium center have no contribution to the HOMO. The HOMO of the proximal arylsulfide complex (see Fig. 3) in general is similar to the distal conformation except for a change in Ti–S–Ar bond angle which causes the titanium d_{z^2} orbital and the overlapping sulfur p-orbital to have different axes.

In the aryloxide HOMO (molecular orbital #70, Fig. 4), the interaction between the oxygen p_y orbital with the coplanar titanium d_{yz} orbital is clearly π-bonding. As in the case of the arylsulfide, the HOMO also includes contributions from π_2 (e_{1g}) phenyl ring orbital and periphery methyl s-orbitals bound to the phenyl ring. The HOMO includes a very weak interaction with the cyclopentadienyl ring and the methyl groups bound to the titanium center.

For the aryloxide, additional O–Ti bonding interactions manifest as one looks at lower energy Kohn–Sham orbitals. In particular, a π-bonding orbital derived from the oxygen p_x interaction with Ti d_{xz} is observed slightly below the Fermi level (orbital #64, Fig. 5), and much deeper in the eigenspectrum (orbital #42, Fig. 6) σ-bonding is evident by the oxygen p_z overlap with the coaxial Ti d_{z^2}. On the other hand in the arylsulfide, aside from the p_z–d_{z^2} σ-bonding in the arylsulfide HOMO, there is a very weak p_x–d_{xz} π-bonding contribution in a slightly lower energy orbital (orbital #76, Fig. 7) for which there is a strong localization around the S atom, leading us to suspect this state is better characterized as a lone pair state. Another S lone pair orbital, p_y, is shown in Fig. 8 (orbital #73).

Bonding analysis

The molecular orbital analysis above provides a bonding picture whereby Ti–arylsulfide bonds are best represented as a single σ-bond with two lone-pair orbitals. Ti–aryloxide bonds seem to be best represented as a triple bond; however, there is a clear preference for electron density to localize on oxygen, suggesting an ionic nature to the interaction. There is still considerable debate as to the representation of the aryloxide bond as covalent or ionic.[32,33] We can extend our DFT analysis to gain a more fundamental insight into the relative importance of ionic *vs.* covalent ligand bonding character in titanium aryloxide and arylsulfide complexes. As a first step, we computed the ionic and covalent dissociation energies as in Table 4:

Dissociation	ΔE/kJ mol^{-1}
$[CpTi(OC_6H_3Me_2\text{-}2,6)Me_2]$ $\rightleftharpoons [CpTiMe_2] + [(OC_6H_3Me_2\text{-}2,6)]$	309
$[CpTi(OC_6H_3Me_2\text{-}2,6)Me_2]$ $\rightleftharpoons [CpTiMe_2]^+ + [(OC_6H_3Me_2\text{-}2,6)]^-$	761
$[CpTi(SC_6H_2Me_3\text{-}2,4,6)Me_2]$ $\rightleftharpoons [CpTiMe_2] + [(SC_6H_2Me_3\text{-}2,4,6)]$	229
$[CpTi(SC_6H_2Me_3\text{-}2,4,6)Me_2]$ $\rightleftharpoons [CpTiMe_2]^+ + [(C_6H_2Me_3\text{-}2,4,6)]^-$	667

These results show that covalent dissociation of the metal–ligand bond into free radicals is much more favorable than ionic dissociation, suggesting that the dissociation of the arylsulfide or aryloxide ligand from the titanium center preferably produces a Ti(III) rather than a Ti(IV) complex.

We also computed the variation of energy as a function of Ti–E–Ar bond angle for $[CpTi(SC_6H_2Me_3\text{-}2,4,6)Me_2]$ and $[CpTi(OC_6H_3Me_2\text{-}2,6)Me_2]$ (Figs. 9 and 10). These were computed by constraining the Ti–E–Ar bond angle and allowing all other structural parameters to relax. In the case of covalent bonding, a Ti–E–C bond angle should reflect the underlying molecular orbital hybridization: ~109° for sp^3 hybridization,

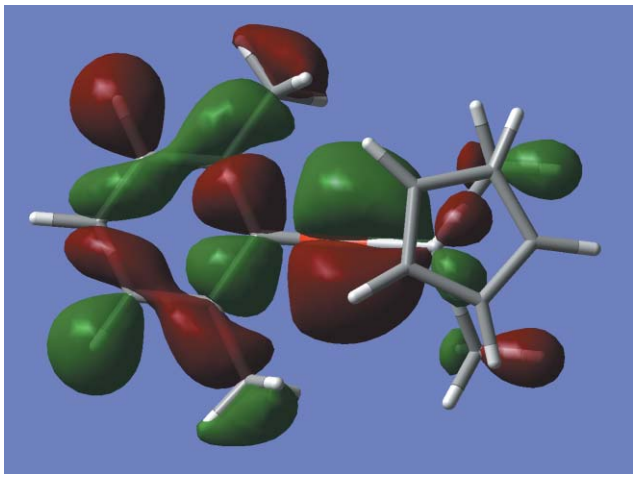

Fig. 5 Molecular orbital #64 of $[CpTi(OC_6H_3Me_2\text{-}2,6)Me_2]$ showing overlap of the oxygen p_x orbital with the titanium d_{xz} orbital.

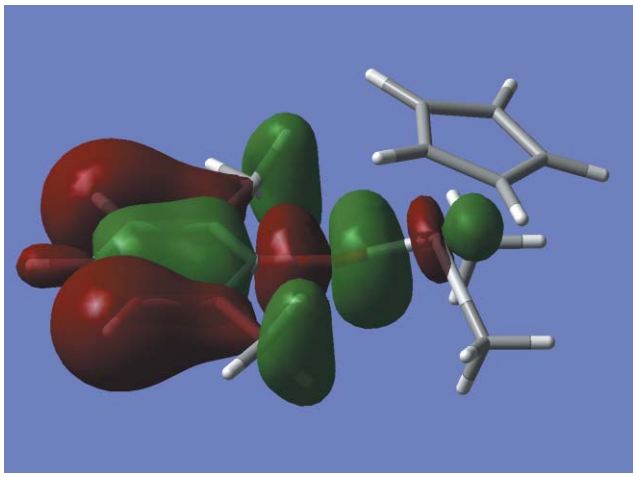

Fig. 6 Molecular orbital #42 of $[CpTi(OC_6H_3Me_2\text{-}2,6)Me_2]$ showing overlap of the oxygen p_z orbital with the titanium d_{z^2} orbital.

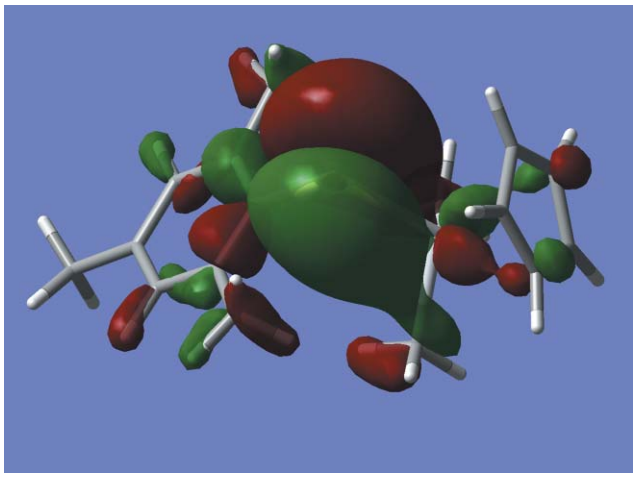

Fig. 7 Molecular orbital #76 of distal $[CpTi(SC_6H_2Me_3\text{-}2,4,6)Me_2]$ showing overlap of the sulfur p_x orbital with the titanium d_{xy} orbital.

~120° for sp^2 hybridization, and ~180° for sp hybridization. The bond angles for the Ti–S–Ar and Ti–O–Ar compounds suggest sulfur sp^3 and oxygen sp hybridization.

We further computed the transition state for conversion from the proximal to distal conformation of $[CpTi(SC_6H_2Me_3\text{-}2,4,6)Me_2]$. The corresponding activation barrier was found to be 29 kJ mol^{-1} with a Ti–S–Ar angle of 132.0° and a Cp–Ti–S–C dihedral angle of −88.2°. We note that conversion of proximal to distal conformation along the lowest energy pathway involves

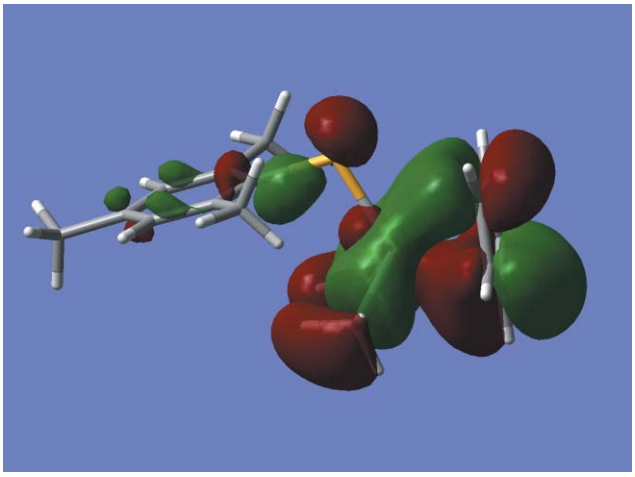

Fig. 8 Non-bonding type interaction between sulfur p_y and titanium in molecular orbital #73 of distal [CpTi($SC_6H_2Me_3$-2,4,6)Me_2].

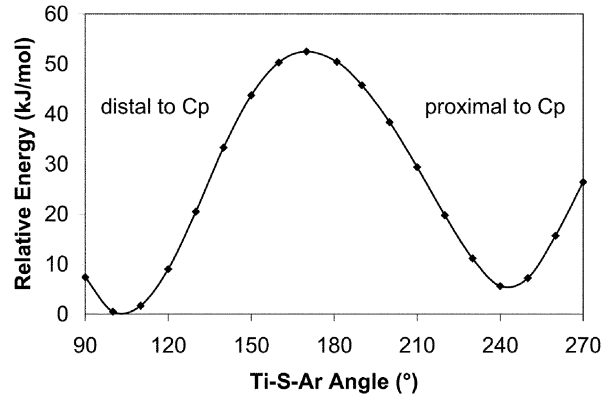

Fig. 9 Variation of energy as a function of Ti–S–Ar angle.

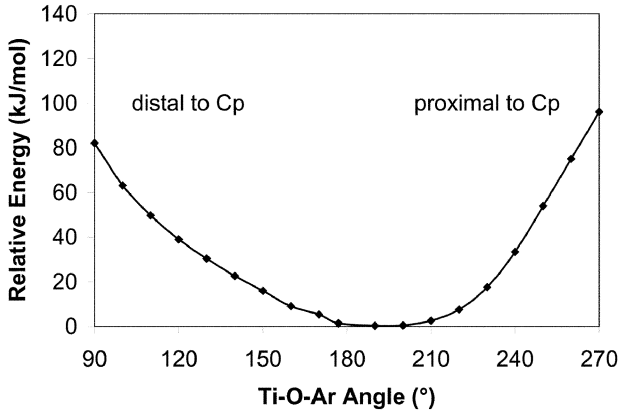

Fig. 10 Variation of energy as a function of Ti–O–Ar angle.

rotation about the Ti–S bond and therefore does not pass through a Ti–S–Ar angle of 180°. Computed geometries for the transition state and several other structures are available in the ESI.† Variable temperature ^{1}H NMR experiments were performed in an attempt to observe the interconversion between proximal and distal conformers. However, this process was not observed *vide infra* (^{1}H NMR) even at temperatures as low as −70 °C. Perhaps the energies of the two conformations are not as close as the calculations suggest leading one form to dominate in solution, or perhaps the interconversion between the two conformations was too rapid for NMR to distinguish them at −70 °C.

The overall order of each titanium-ligand bond was computed in Gaussian 03 using the Wiberg bond index array,[34] for which we quote, "the elements of this array are the sums of squares of off-diagonal density matrix elements between pairs of atoms in the NAO basis, and are the NAO counterpart of the Wiberg bond index."[35]

The Wiberg method for [CpTi($OC_6H_3Me_2$-2,6)Me_2] gives a Ti–O bond index of 0.76, an O–Ar bond index of 1.00, a Ti–Me bond index of 0.80, and a Ti–C bond index of 0.19–0.22 for each of the cyclopentadienyl carbons giving a Ti–Cp bond index of 1.00. Overall, it gives a total bond index of 3.66 for Ti, which is consistent with the observation that Ti has four electrons to share.

The Wiberg method for distal [CpTi($SC_6H_2Me_3$-2,4,6)Me_2] gives a Ti–S bond index of 1.05, a S–Ar bond index of 1.02, a Ti–Me bond index of 0.79, and a Ti–C bond index of 0.20–0.24 for each of the cyclopentadienyl carbons giving a Ti–Cp bond index of 1.09. Overall, we observe a total bond index of 4.02 for Ti, which is also consistent with the observation that Ti has four electrons to share.

Natural bond order (NBO)[35] analysis was used to generate Lewis structures for the above compounds. We generated the Lewis structure of Fig. 11(a) for the arylsulfide compounds while we generated the ionic form of Fig. 11(b) for the aryloxide compound.

Taking all of the above information into account, a consistent picture emerges for the differences in bonding between titanium arylsulfide and aryloxide complexes. The arylsulfides can be adequately represented by the Lewis structure of Fig. 11(a). This structure predicts a Ti–S–Ar angle of approximately 109° and a Ti–S bond order of one. We also predicted the two different configurations, proximal and distal, that the molecule can adopt. On the other hand, the aryloxides cannot be adequately represented by a single Lewis structure, but may be represented by the resonance forms depicted in Fig. 11(b). Note that this resonance predicts a nearly linear Ti–O–Ar bond angle, interaction through all three oxygen p orbitals, and an overall Ti–O covalent bond index of one.

These observations can be rationalized as following based on the molecular orbitals. The sulfur and oxygen atoms each have three p orbitals which may overlap with d orbitals on titanium. In the case of sulfur, one of the interactions is strong (Figs. 2–3), while two of the interactions are very weak (Figs. 7–8). In the case of oxygen, all three of the interactions are moderately weak (Figs. 4–6). As a result, the geometry in the arylsulfide complexes changes to optimize the strength of the one strong interaction at the expense of the two very weak interactions giving a bent Ti–S–Ar. In the case of aryloxide, the geometry optimizes to simultaneously optimize the strength of all three moderately weak interactions.

Our experience with computations of the geometries of similar titanium aryloxide and arylsulfide complexes have indicated similar bonding to the compounds presented here. Cationic complexes [$Ti(OAr)_2Me^+$] and [CpTi(OAr)Me^+], cation-anion

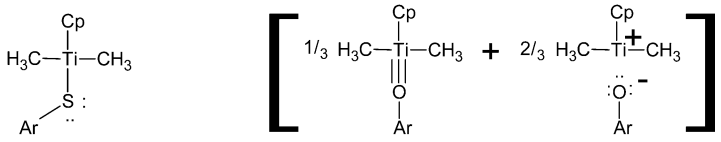

(a) **(b)**

Fig. 11 Lewis structures of (a) CpTi(SAr)Me_2 and (b) CpTi(OAr)Me_2.

complexes $[Ti(OAr)_2Me^+][MeB(C_6F_5)_3^-]$ and $[CpTi(OAr)Me^+][MeB(C_6F_5)_3^-]$, and neutral complexes $[Ti(OAr)_2Me_2]$ and $[CpTi(OAr)Me_2]$ have all been found to have similar metal ligand bonding, though small differences occur in bond distances and angles.

Conclusions

The titanium arylsulfide ligand bond is primarily a covalent sp^3 hybridized single bond with two lone pairs residing on the sulfur atom. DFT calculations suggest that $[CpTi(SC_6H_2Me_3\text{-}2,4,6)Me_2]$ can exist in two conformations as proximal and distal, although only the distal conformation was observed in solid state. Conversion between the two conformations occurs readily with an activation energy barrier of approximately 29 kJ mol^{-1}. However, this interconversion was unobservable *vide infra* (^1H NMR) even at −70 °C.

In contrast to the titanium arylsulfide bond, the titanium aryloxide bond is primarily sp hybridized, and three of the oxygen lone pairs interact weakly with the titanium metal center. This creates a bond which is a resonance between a covalent triple bond and an ionic bond. In both the arylsulfide and aryloxide compounds, the overall Ti–E bond order is nearly one. And in both compounds, covalent dissociation of the bond is energetically preferred over ionic dissociation.

Acknowledgements

Support for this research was provided by the U.S. Department of Energy, Office of Basic Energy Sciences, through the Catalysis Science Grant No. DE-FG02-03ER15466. Computational resources were obtained in part from the Purdue IBM Supercomputing Cluster—part of the Information and Technology at Purdue (ITaP)—and through a grant from the National Center for Supercomputing Applications (NCSA).

References

1 G. Wilkinson and J. L. Birmingham, *J. Am. Chem. Soc.*, 1954, **76**, 4281.
2 G. Wilkinson, P. L. Puason, J. L. Birmingham and F. A. Cotton, *J. Am. Chem. Soc.*, 1953, **75**, 15.
3 A. Togni and R. L. Halterman, in *Metallocenes: Synthesis, Reactivity, Applications*, Wiley-VCH, Weinheim, Germany, 1998.
4 Y. Zhang, E. K. Reeder, R. J. Keaton and L. R. Sita, *Organometallics*, 2004, **23**, 3512.
5 M. G. Thorn, Z. C. Etheridge, P. E. Fanwick and I. P. Rothwell, *J. Organomet. Chem.*, 1999, **591**, 148.
6 M. G. Thorn, Z. C. Etheridge, P. E. Fanwick and I. P. Rothwell, *Organometallics*, 1998, **17**, 3636.
7 K. Nomura, N. Naga, M. Miki, K. Yanagi and A. Imai, *Organometallics*, 1998, **17**, 2152.
8 M. G. Thorn, J. S. Vilardo, J. Lee, B. Hanna, P. E. Fanwick and I. P. Rothwell, *Organometallics*, 2000, **19**, 5636.
9 A. E. Fenwick, K. Phomphrai, M. G. Thorn, J. S. Vilardo, C. A. Trefun, B. Hanna, P. E. Fanwick and I. P. Rothwell, *Organometallics*, 2004, **23**, 2146.
10 K. Pomphrai, A. E. Fenwick, S. Sharma, J. M. Caruthers, W. N. Delgass and I. P. Rothwell, in preparation.
11 A. E. Fenwick, P. E. Fanwick and I. P. Rothwell, *Organometallics*, 2003, **22**, 535.
12 P. T. Bishop, J. R. Dilworth, T. Nicholson and J. A. Zubieta, *J. Chem. Soc., Dalton Trans.*, 1991, 385.
13 P. J. Blower, J. R. Dilworth, J. Hutchinson, T. Nicholson and J. A. Zubieta, *J. Chem. Soc., Dalton Trans.*, 1985, 2639.
14 K. Ruhlandt-Senge and P. P. Power, *Bull. Soc. Chim. Fr.*, 1992, **129**, 594.
15 R. R. Schrock, M. Wesolek, A. H. Liu, K. C. Wallace and J. C. Dewan, *Inorg. Chem.*, 1988, **27**, 2050.
16 J. J. Ellison, K. Ruhlandt-Senge and P. P. Power, *Angew. Chem., Int. Ed. Engl.*, 1994, **33**, 1178.
17 K. Look and R. K. Norris, *Aust. J. Chem.*, 1999, **52**, 1077.
18 F. A. Cotton and W. A. Wojtczak, *Gazz. Chim. Ital.*, 1993, **123**, 499.
19 M. J. Frisch, G. W. Trucks, H. B. Schlegel, G. E. Scuseria, M. A. Robb, J. R. Cheeseman, J. J. A. Montgomery, T. Vreven, K. N. Kudin, J. C. Burant, J. M. Millam, S. S. Iyengar, J. Tomasi, V. Barone, B. Mennucci, M. Cossi, G. Scalmani, N. Rega, G. A. Petersson, H. Nakatsuji, M. Hada, M. Ehara, K. Toyota, R. Fukuda, J. Hasegawa, M. Ishida, T. Nakajima, Y. Honda, O. Kitao, H. Nakai, M. Klene, X. Li, J. E. Knox, H. P. Hratchian, J. B. Cross, C. Adamo, J. Jaramillo, R. Gomperts, R. E. Stratmann, O. Yazyev, A. J. Austin, R. Cammi, C. Pomelli, J. W. Ochterski, P. Y. Ayala, K. Morokuma, G. A. Voth, P. Salvador, J. J. Dannenberg, V. G. Zakrzewski, S. Dapprich, A. D. Daniels, M. C. Strain, O. Farkas, D. K. Malick, A. D. Rabuck, K. Raghavachari, J. B. Foresman, J. V. Ortiz, Q. Cui, A. G. Baboul, S. Clifford, J. Cioslowski, B. B. Stefanov, G. Liu, A. Liashenko, P. Piskorz, I. Komaromi, R. L. Martin, D. J. Fox, T. Keith, M. A. Al-Laham, C. Y. Peng, A. Nanayakkara, M. Challacombe, P. M. W. Gill, B. Johnson, W. Chen, M. W. Wong, C. Gonzalez, and J. A. Pople, in *Gaussian 03*, Pittsburgh PA, 2003.
20 A. Frisch, M. J. Frisch, and G. W. Trucks, *Gaussian 03 User's Reference*, Gaussian Inc., 2003.
21 N. C. Handy and A. J. Cohen, *Mol. Phys.*, 2001, **99**, 403.
22 C. T. Lee, W. T. Yang and R. G. Parr, *Phys. Rev. B*, 1988, **37**, 785.
23 J. Baker and P. Pulay, *J. Chem. Phys.*, 2002, **117**, 1441.
24 P. C. McArdle, *J. Appl. Crystallogr.*, 1996, **29**, 306.
25 Z. Otwinowski and W. Minor, Processing of X-ray Diffraction Data Collected in Oscillation Mode, *Methods in Enzymology: Macromolecular Crystallography, Part A*, ed. C. W. Carter, Jr. and R. M. Sweet, Academic Press, New York, 1997, vol. 276, pp. 307–326.
26 P. T. Beurskens, G. Admiraal, G. Beurskens, W. P. Bosman, S. Garcia-Granda, R. O. Gould, J. M. Smits and C. Smykalla, *The DIRDIF92 Program System; Technical Report*, Crystallography Laboratory, University of Nijmegen, Nijmegen, The Netherlands, 1992.
27 *International Tables for Crystallography*, Kluwer Academic, Dordrecht, 1992.
28 G. M. Sheldrick, *SHELXS-97, Program for solution of crystal structures*, University of Göttingen, Germany, 1997.
29 L. J. Farrugia, *J. Appl. Crystallogr.*, 1997, **30**, 565.
30 J. C. Slater, *J. Chem. Phys.*, 1964, **39**, 3199.
31 G. D. Smith, P. E. Fanwick and I. P. Rothwell, *Inorg. Chem.*, 1990, **29**, 3221.
32 D. C. Bradley, I. P. Mehrotra, I. P. Rothwell and A. Singh, *Alkoxo and Aryloxo Derivatives of Metals*, Academic Press, 2001.
33 M. R. Russo, N. Kaltsoyannis and A. Sella, *Chem. Commun.*, 2002, 2458.
34 K. Wiberg, *Tetrahedron*, 1968, **24**, 1083.
35 E. D. Glendening, A. E. Reed, J. E. Carpenter, and F. Weinhold, *NBO 3.0 Program Manual*, University of Wisconsin, 1996.